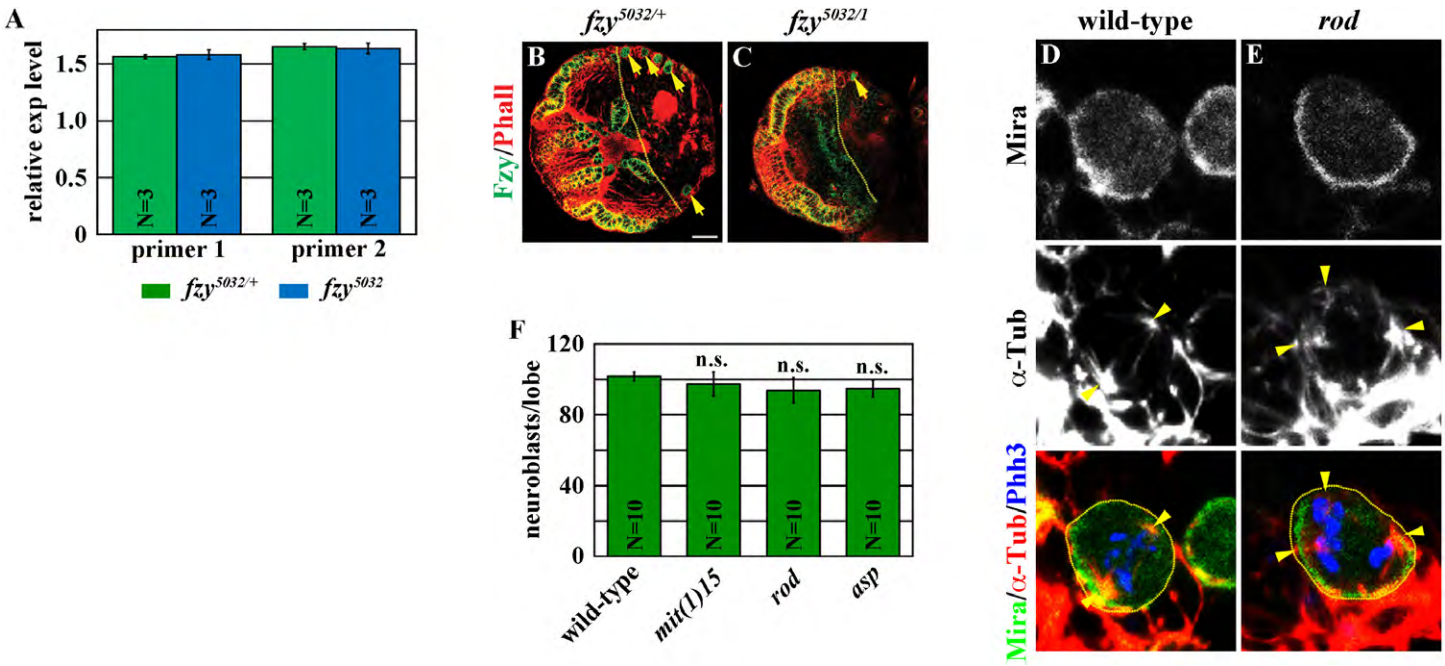

Fig. S1 The *fzy*^{5032} mutation perturbs the function of Fzy in the maintenance of neuroblasts.

(**A**) The *fzy*^{5032} mutation does not reduce the level of *fzy* transcript. The relative expression level of *fzy* mRNA to *rp49* mRNA in control or *fzy*^{5032} larvae was shown (N = 3 reactions per genotype).

(**B-C**) The *fzy*^{5032} mutation does not affect Fzy protein expression. Brains from larvae of the indicated genotype aged for 96 hours after hatching were stained for Fzy and Phall. Scale bar, 20mm.

(D-F) Defective chromosome segregation is not sufficient to induce premature neuroblast loss. Brains from larvae of the indicated genotype aged for 96 hours after hatching were stained for Miranda (Mira), α-Tubulin and phosphorylated histone H3. A wild-type anaphase neuroblast showed asymmetric localization of Mira and possessed two spindle poles (yellow arrowheads). A *rod* mutant anaphase neuroblast showed expanded localization of Mira and possessed multiple spindle poles (yellow arrowheads). (F) The average number of neuroblasts per brain lobe is shown.

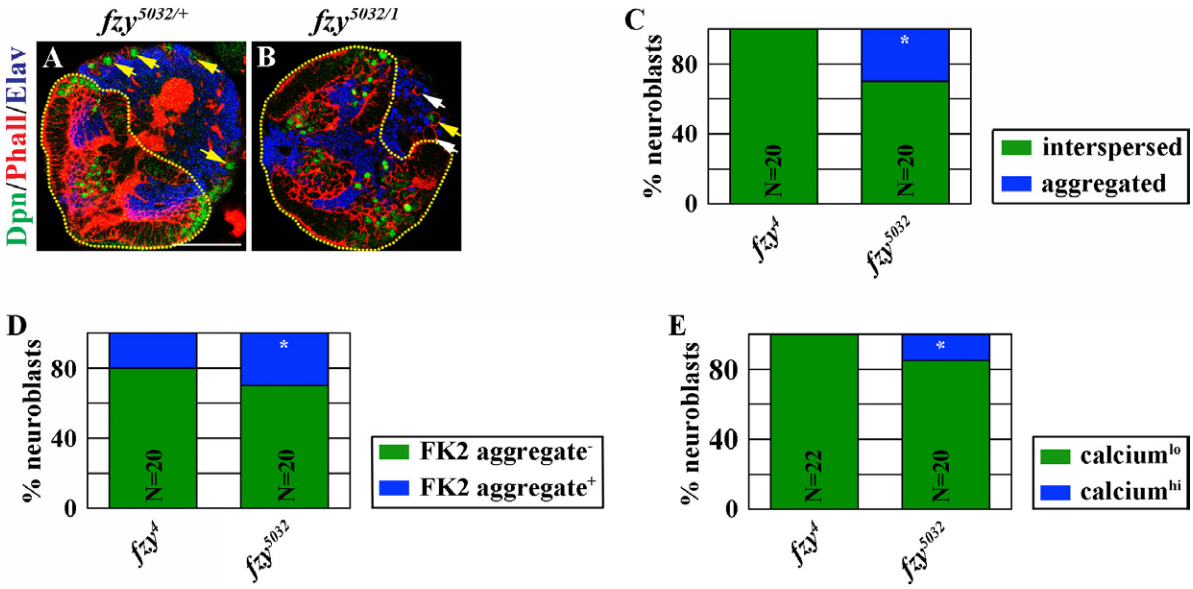

Fig. S2 Neuroblast loss in *fzy* null brains mainly occurs through defects in cell cycle regulation.

(**A-B**) Neuroblasts in *fzy*^{5032} brains never expressed the neuronal marker. Brains from larvae of the indicated genotype aged for 96 hours after hatching were processed to stain with the neuronal marker Elav. Scale bar, 20mm.

(**C-E**) Cell cycle function of Fzy is dominant in contributing to neuroblast loss. Larvae containing GFP-marked mosaic clones derived from single neuroblasts of the indicated genotypes were aged for 72 hours after clone induction, and brains were processed for staining with ATP5a (C), FK2 (D) and GFP (E). The percentage of neuroblasts with (blue) or without (green) the expression of the indicated marker is shown.

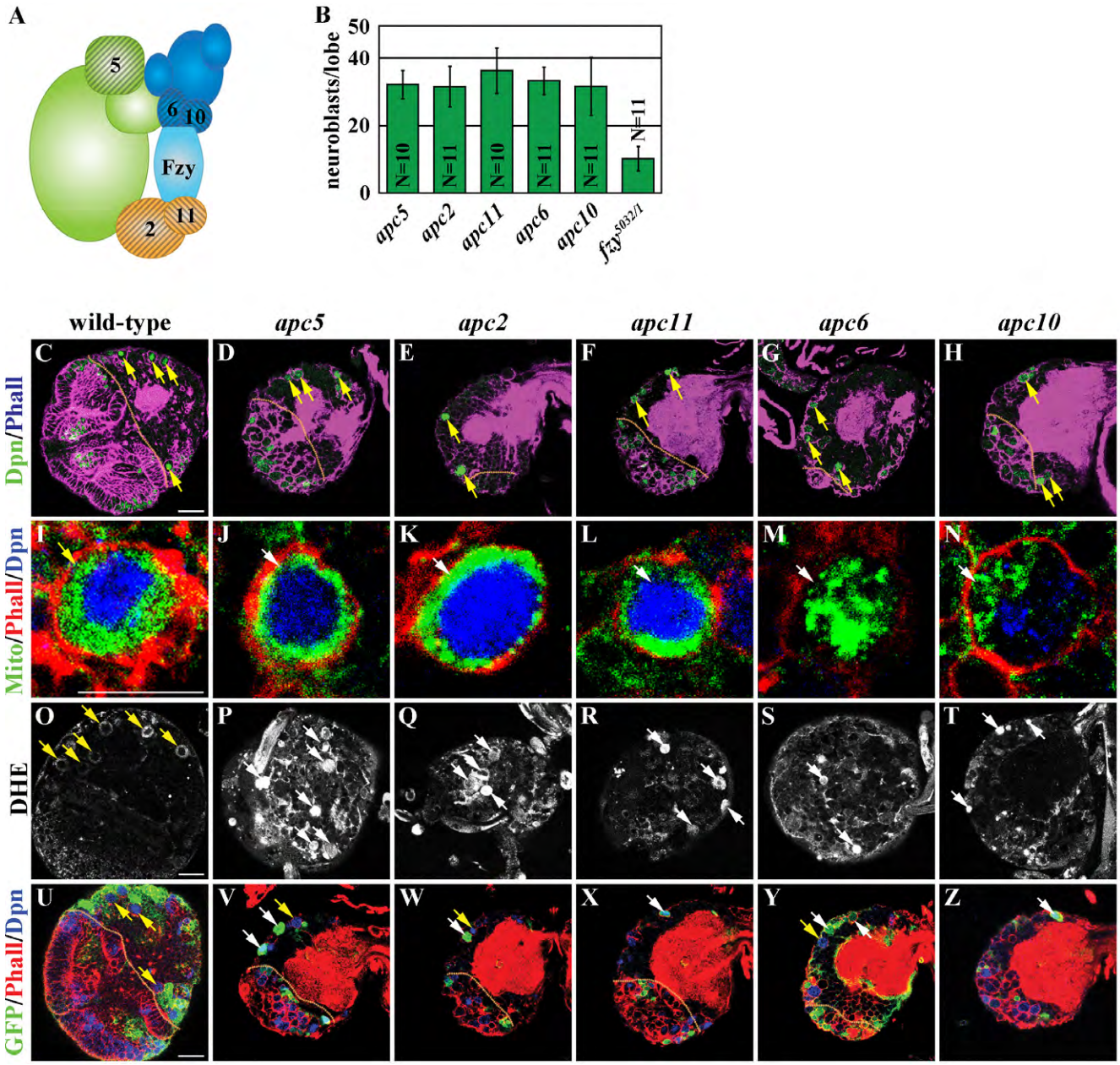

Fig. S3 Neuroblasts lacking APC/C function undergo necrosis.

(**A**) Summary diagram of the APC/C-Fzy complex. Scaffold subunits (green); catalytic subunits (orange); substrate recruitment subunits (blue). Crosshatches mark subunits whose mutants were analyzed.

(**B**) Brains lacking APC/C function showed neuroblast loss. The average number of neuroblasts per brain lobe in larvae of the indicated genotypes is shown.

(**C-Z**) Neuroblasts in larval brains mutant for the subunit of APC/C exhibited necrosis markers. Brains from larvae of the indicated genotype were processed for staining with (C-H) Dpn (Scale bar, 20mm), (I-N) ATP5a (Scale bar, 10mm), (O-T) DHE (Scale bar, 20mm), (U-Z) GFP (Scale bar, 20mm).

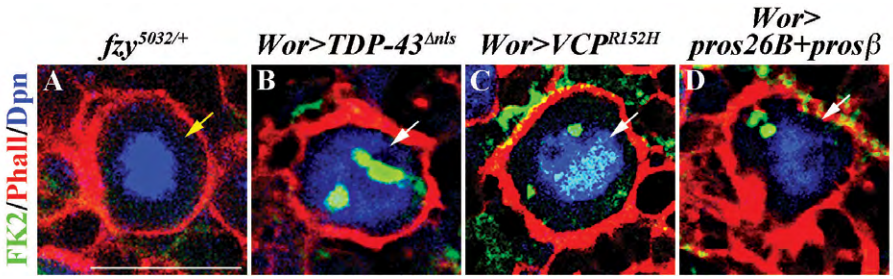

Fig. S4 Over-expression of toxic proteins or reduction in proteasome function led to aberrant accumulation of ubiquitin-conjugated aggregates in neuroblasts.

(A-D) Neuroblasts over-expressing toxic proteins or showing reduced proteasome function showed aberrant accumulation of ubiquitin-conjugated aggregates. Brains from larvae of the indicated genotype aged for 72 hours after hatching were stained for FK2. Scale bar, 10mm.

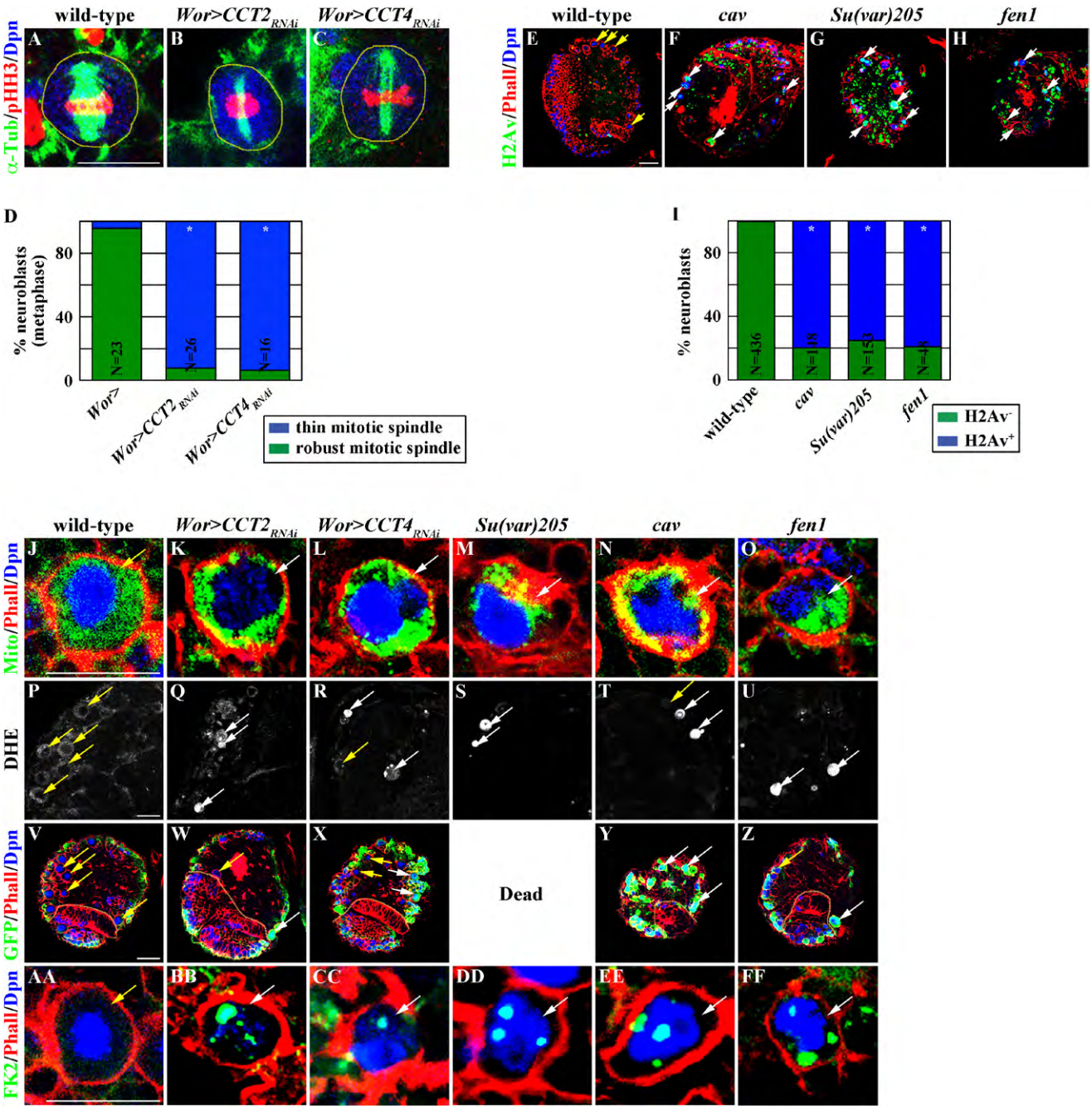

Fig. S5 Neuroblasts experiencing catastrophic cellular stress undergo necrosis.

(**A-D**) Reduced function of the CCT chaperonin complex decreased α-Tubulin expression in mitotic neuroblasts. (A-C) Brains from larvae of the indicated genotype aged for 72 hours after hatching were stained for α-Tubulin, phosphorylated histone H3 and Dpn. Scale bar, 10mm. (D) The percentage of metaphase neuroblasts possessing a thin (blue) or a robust (green) mitotic spindle is shown.

(**E-I**) Removing the function of the telomere capping protein complex or Fen1 endonuclease led to an increase in DNA damage response. (E-H) Brains from larvae of the indicated genotype aged for 72 hours after hatching were stained for DNA damage marker phosphorylated histone H2Av. Scale bar, 20mm. (I) The percentage of neuroblasts with (blue) or without (green) the expression of phosphorylated

histone H2Av is shown.

(**J-FF**) Neuroblasts experiencing catastrophic cellular stress displayed necrosis markers. Brains from larvae of the indicated genotype were processed for staining with (J-O) ATP5a (Scale bar, 10mm), (P-U) DHE (Scale bar, 20mm), (V-Z) GFP (Scale bar, 20mm) and (AA-FF) FK2 (Scale bar, 10mm).

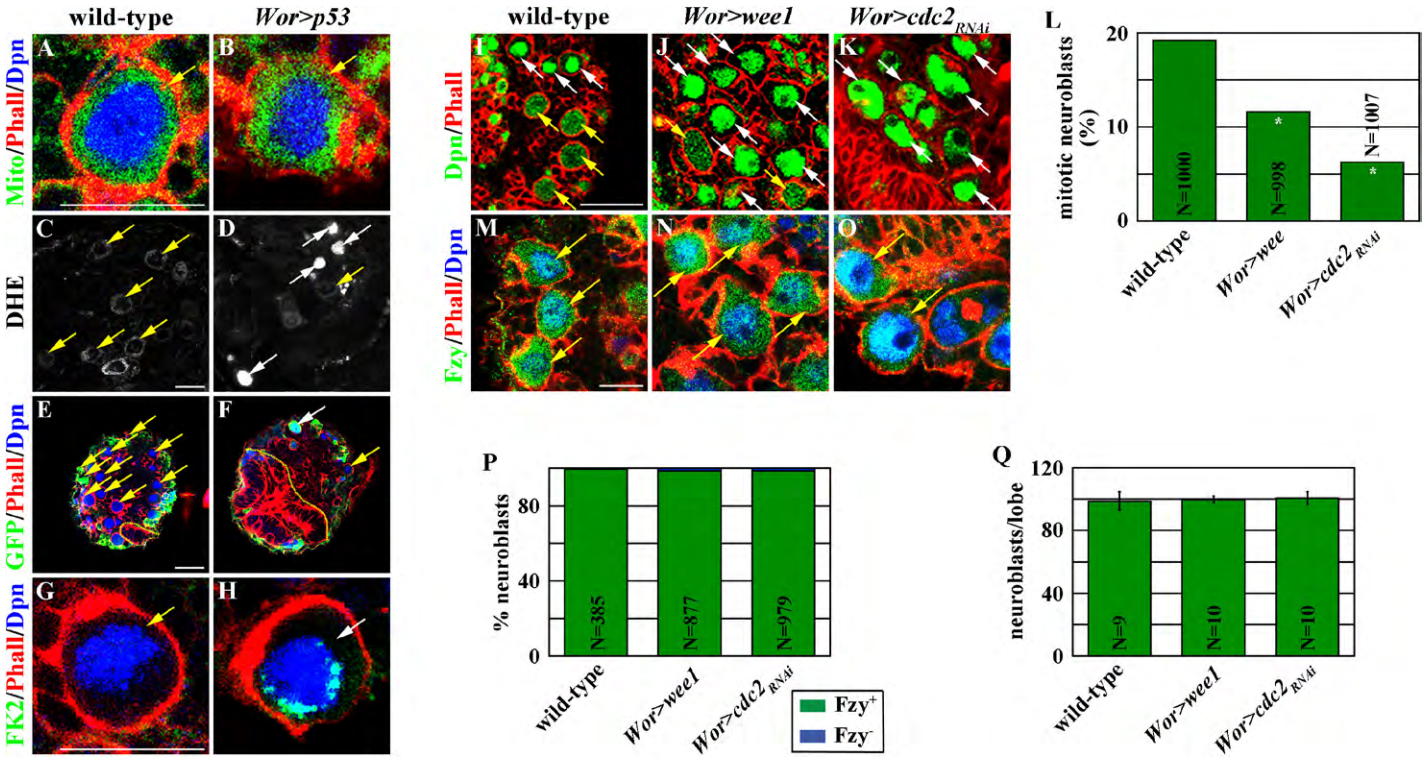

Fig. S6 Neuroblasts over-expressing *p53* undergo necrosis.

(**A-H**) Neuroblasts over-expressing p53 displayed the expression of necrotic markers. Brains from larvae of the indicated genotype were processed for staining with (A-B) ATP5a (Scale bar, 10mm), (C-D) DHE (Scale bar, 20mm), (E-F) GFP (Scale bar, 20mm), (G-H) FK2 (Scale bar, 10mm).

(**I-Q**) Increased function of *wee1* or decreased function of *cdc2* induced G2 cell cycle arrest in neuroblasts. (I-L) Over-expression of *wee1* or reduction in *cdc2* led to a decrease in mitotic neuroblasts and an increase in neuroblast diameter. Scale bar, 20mm. (L) The percentage of neuroblasts in mitosis is shown. (M-P) Over-expression of *wee1* or reduction in *cdc2* function did not abolish Fzy protein expression. Scale bar, 10mm. (Q) The average number of neuroblasts per brain lobe is shown.

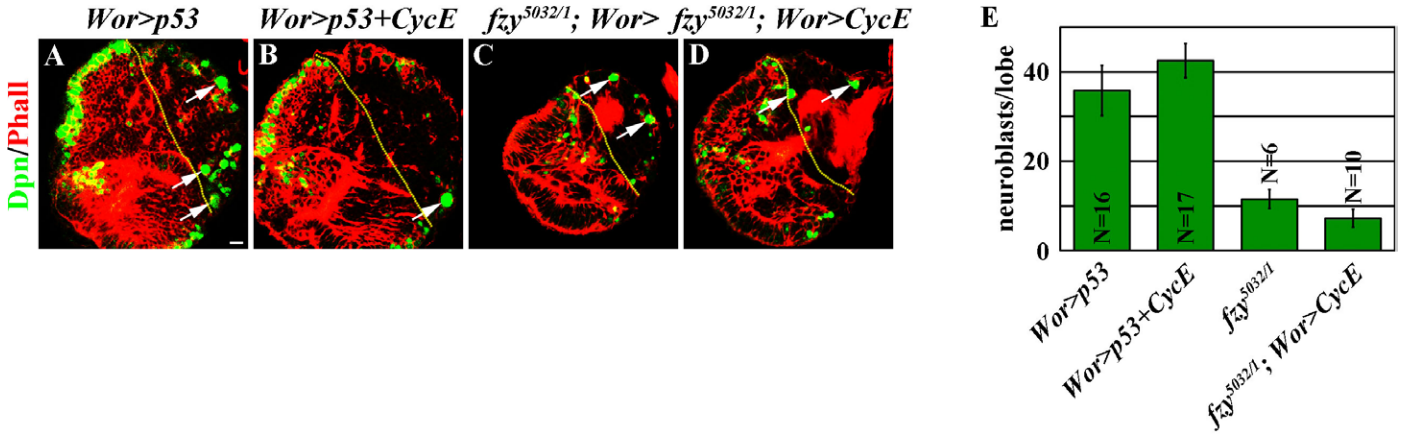

Fig. S7 Over-expression of Cyclin E did not suppress the necrosis of neuroblasts in *fzy*^{5032} brains.

(**A-E**) Necrosis of neuroblasts induced by over-expression of *p53* or the *fzy*^{5032} mutation occurs independently of Cyclin E. (A-D) Brains from larvae of the indicated genotype were processed for staining with the indicated markers. Scale bar, 10mm. (E) The average number of neuroblasts per brain lobe is shown.